Stripped Bed Roughness Effect on Flow Measurement in Trapezoidal Channels with Free Overfalls

Safa S. Ibrahim
Petroleum Engineering Department,
Assistant Lecturer
Zakho, Iraq
safa.subhi@uod.ac

Dr. Bahzad M. A. Noori
Civil Engineering Department
Assistant Professor
Dohuk, Iraq
bahzadn@yahoo.com

Abstract- **The aim of the present investigation is to study the effects of side slope, bed slope and bed roughness on the flow over free overfalls in trapezoidal channels. Three models of trapezoidal free overfall channels have been built and tested in a laboratory flume; each model had four different bed slopes. For each slope, the bed was roughened using artificial strip roughness elements with eight different roughness patterns. The experimental testing program included ninety-six series of experiments for different ranges of Froude number. Experimental results of all models showed that the variation of ($Qm^{1.5}/\sqrt{gb^5}$) with (my_b/b) for different bed slopes and various roughness patterns is simple power equation. It was also observed that values of ($Qm^{1.5}/\sqrt{gb^5}$) increase with the increase of (my_b/b) values. The correlation between (my_b/b) with (my_c/b) was found to be linear for different bed slopes and roughness patterns. The ratio (y_b/y_c) decreases with the increase of bed slope (S). An empirical expression was obtained for the variation of ($Qm^{1.5}/\sqrt{gb^5}$) with (my_b/b) and (S/n) for the free overfalls with rough beds.**

Keywords- Flow measurement; stripped bed roughness; trapezoidal channesl, free overfalls.

I. INTRODUCTION

A free overfall represents a vertical fully aerated drop at the downstream portion of a channel. It is the simplest case of weir flow having zero weir height with no submergence [1]. The free overfall has a distinct importance in hydraulic engineering; it forms the starting point in computations of the surface in a gradually varied flow; such as the discharge spills into an open reservoir at the downstream end. The study of a free overfall is also important because it can be used as a discharge measuring device [2]. In the past, there were many attempts trying to obtain a relation between the brink depth and the discharge in channels and to investigate the effects of different shapes of the channel cross section on the free overfall depending on the flow conditions, approach channel slope and bed roughness. Since then, many investigators have investigated the effects of the bed slope and bed roughness on the EDR (EDR = end depth (y_b) / critical depth (y_c)) in different shapes of the channels such as: Rouse [3], Delleur et al. [4], Rajartnam et al. [5], Davis et al [6], Dey [7-11], Ferro [12], Ahmad [13], Gue et al [14], Tigrek et al. [15], Mohammed et al [16], and Vantankah [17]. On the other hand, investigations on the free overfall in a trapezoidal channel are relatively few. The earliest significant study was performed by Diskin [18] who carried out measurements for a supercritical flow in a trapezoidal channel. Hamid [19] experimentally and theoretically studied the trapezoidal free overfall. In these investigations, the momentum equation was solved assuming a zero pressure distribution at the brink section. Keller and Fong [20] experimentally and theoretically studied the trapezoidal free overfall. An appropriate assumption for the pressure distribution at the free overfall was made, based on available measurements in rectangular and triangular channels. They derived a sixth-degree equation linking the end depth to the critical depth. Terzidis and Anastasiadou-Partheniou [21], looking at the trapezoidal section in the same way of Keller and Fong [20] and using Replogle's [22] and Rajaratnam and Muralidhar [23] measurements, derived a very simple equation linking the end-depth and the critical depth. Gupta et al. [24] statistically analyzed published experimental data and provided a calibration curve using dimensionless parameters for the prediction of discharge with the brink depth in smooth trapezoidal overfall channels with different bed slopes. They found that $X_b/X_c = 0.745$ and 0.726 ($X_c = my_c/b$ and $X_b = my_b/b$, where m is the side slope (m horizontal to 1 vertical), and b is the base width) for horizontal and positive slope channels, respectively. Bhallamudi [25] analytically determined the end depth in trapezoidal and exponential channels using the momentum approach and the Boussinesq approximation and estimated the discharge using the end depth measurement. The momentum equation incorporating the effect of streamline curvature was also used to obtain the non-dimensional water surface profiles in front of a free overfall. Anastasiadou-Partheniou and Hatzigiannakis [26] presented the flow over a fall in trapezoidal channels and simulated it with a sharp crested weir. A general end-depth-discharge relationship, for both subcritical and supercritical flow, was obtained.

From the extensive literature survey carried out for the previous studies, one may clearly conclude that very few works have been carried out and published in the past dealing with the free-fall of trapezoidal channels. Accordingly, the writers have brought this problem to light and studied the effects of bed slope and bed roughness on the hydraulic characteristics of free

overfalls of trapezoidal channels. Also, the present investigation aims to provide relationships for the estimation of flow rate using brink depth and taking into account different effective parameters expected to affect the discharge measurements in free-fall of trapezoidal rough channels.

II. THEORY

A. Momentum Equation for End Depth Flow

With reference to Fig. 1 and applying the momentum equation to the control volume between sections A and B, according to Keller and Fong [20], yields:

$$Q\rho V_b - Q\rho V_c = F_c - F_b \quad (1)$$

in which, Q is the flow rate, ρ is the mass density of fluid, V is velocity, F is horizontal force, and subscripts b and c refer to the end section and the critical section, respectively. Introducing the horizontal forces F_c and F_b in Eq. (1), gets:

$$F_c = \gamma(A\bar{y})_c \quad (2)$$

$$F_b = K\gamma(A\bar{y})_b \quad (3)$$

in which, K is pressure factor, γ is the fluid specific weight, A is cross sectional area, and $\bar{y}$ is the depth from the flow surface to the centroid of flow cross section. The relation between the discharge and critical depth can be written as:

$$\frac{Q^2}{g} = \frac{A_c^3}{T_c} \quad (4)$$

where, g = acceleration due to gravity and T_c = the surface top width. Substituting Equations (2), (3) and (4) (using $V = Q/A$ and $\gamma = \rho g$) into Eq. (1) and rearranging yields:

$$\frac{A_c}{T_c}\left[\frac{A_c^2}{A_b} - A_c\right] = (A\bar{y})_c - K(A\bar{y})_b \quad (5)$$

By simple application of moments to a trapezoidal cross section yields:

$$\bar{y} = \frac{(3+2X)}{6(1+X)}y \quad (6)$$

$$\frac{A}{T} = \frac{(1+X)}{(1+2X)}y \quad (7)$$

in which, $X = my/b$. (where m is the side slope (m horizontal to 1 vertical), y is the depth of water at any section and b is the base width)). Substituting Eqs. (6) and (7) with appropriate subscripts into Eq. (5) and after rearranging yields:

$$10X_c^4 + 20X_c^3 + 9X_c^2 - \frac{6}{G_1}(X_c^3 + 3X_c^4 + 3X_c^5 + X_c^6) - K\,G_1G_2(1+2X_c) = 0 \quad (8)$$

in which, $G_1 = X_b + X_b^2$ and $G_2 = \frac{(3+2X_b)X_b}{(1+X_b)}$. (where: $X_c = my_c/b$ and $X_b = my_b/b$). Eq. (8) links the depth at the end section to the critical depth.

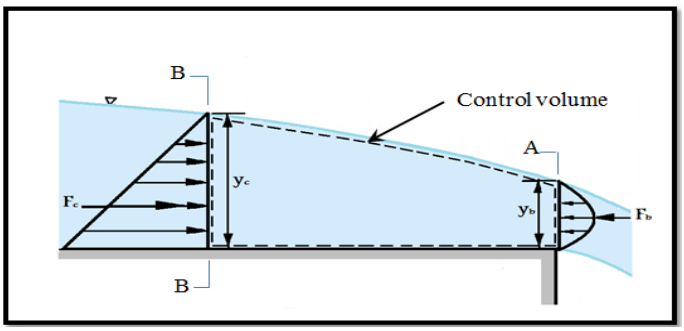

Figure 1. Control volume for theoretical analysis

B. Critical Depth in a Trapezoidal Channel

Critical depth depends only on the discharge rate and the channel geometry. The critical state of flow through a channel section is characterized by several important conditions: The specific energy and specific force are minimum for the given discharge. The Froude number is equal to unity. For a given specific energy, the discharge is maximum at the critical flow. The velocity head is equal to half the hydraulic depth in a channel, Das [27]. Substituting the parameters of $A_c = by_c + my_c^2$ and $T_c = b + 2my_c$ into Eq. (4) and after rearranging yields:

$$m^3y_c^6 + 3bm^2y_c^5 + 3b^2my_c^4 + b^3y_c^3 - 2my_c\frac{Q^2}{g} - \frac{Q^2}{g}b = 0 \quad (9)$$

In the present study, the critical depth in Eq. (9) can be solved for any given values of m, b, and Q.

C. Depth Measurements

Flow along rough boundary is not uniform in the exact sense as the depth varies in the flow direction. In order to apply the approximation of uniform flow conditions, it has to be decided at which height the bed level should be chosen with respect to which the flow depth is to be measured. Schlichting [28] introduced the concept of geometric bed level that would arise if all the roughness elements were melted to form a smooth surface and using this level as a reference datum. Morris [29] has adopted the top of the roughness as a datum or level of the theoretical bed. Gordienko [30] has concluded that the designed depth is greater than the depth above roughness crest but smaller than the depth down to the bottom of the flume ye < y < ye+h (where: y_e is the flow depth measured from the crests of roughness elements, and h is the height of roughness element). In the present study, the geometric mean bed level has been adopted as a datum for the measurements of normal depths upstream of the brink section.

D. Manning's Roughness Coefficient

The estimation of roughness coefficient and discharge capacity in a channel or in a river is one of the most fundamental problems facing river engineering. Therefore, in this study the Manning's roughness coefficient is one of the main variables which affects the flow behavior at brink section; the well-known Manning's formula is used as:

$$n = \frac{R^{2/3} S^{1/2}}{Q/A} \quad (10)$$

in which, n = Manning's roughness coefficient, R = hydraulic radius = A/Pw, A = flow area, Pw= wetted perimeter, and S = slope of the energy grade line, which is taken identical to the channel bottom slope in uniform flow.

E. Dimensional Analysis

The flow in a trapezoidal free overfall channels with roughness elements is expected to be a function of the following variables:

$$Q = f_1(y_b, S, b, m, g, \rho, \mu, n, \mathrm{V}) \quad (11)$$

in which, Q = flow rate (L^3T^{-1}), y_b = brink depth (L), S = bed slope of the channel, b = channel width (L), m = channel side slope (m horizontal to 1 vertical), g = acceleration due to gravity (LT^{-2}), ρ = mass density of water (ML^{-3}), μ = viscosity of water ($MT^{-1}L^{-1}$), n = Manning's roughness coefficient, and V = flow velocity (LT^{-1}). According to Chow [31], n is assumed to be dimensionless. Using the Buckingham's Pi-theorem, and selecting b, V, and ρ as repeating variables, Eq. (11) becomes:

$$f_2\left(\frac{y_b}{b}, \frac{Q}{Vb^2}, Re, \frac{V^2}{gb}, n, S, m\right) = constant \quad (12)$$

in which, Re = Reynolds number. During the experimental program, Reynolds number (Re) range varied from 3358 to 46392, the flow was turbulent and the viscous forces were weak relative to the inertial forces. Therefore, the flow is assumed to be independent of (Re) (Chow [31]) and (Re) can be dropped from Eq. (12). Rearranging Eq. (12), taking (S/n) and using mathematical operations for obtaining new dimensionless parameters:

$$\frac{Q}{Vb^2} * \frac{Vm^{1.5}}{\sqrt{gb}} = \frac{Qm^{1.5}}{\sqrt{gb^5}} \quad (13)$$

Eq. (12) can be reduced to the form:

$$\frac{Qm^{1.5}}{\sqrt{gb^5}} = f_3\left(\frac{my_b}{b}, \frac{S}{n}\right) \quad (14)$$

Substituting A_c and T_c into Eq. (4) and writing in terms of the base width b, side slope m, and critical depth y_c, and rearranging yields:

$$\frac{Qm^{1.5}}{\sqrt{gb^5}} = \sqrt{\frac{(1 + X_c)^3}{(b + 2X_c)}} = f(X_c) \quad (15)$$

Since, through Eq. (8), $X_c = my_c/b$ is a function of $X_b = my_b/b$, therefore Eq. (14) can be written in a functional form as:

$$\frac{my_b}{b} = f_4\left(\frac{my_c}{b}, S, n\right) \quad (16)$$

III. MATERIALS AND METHODS

A. Experimental Setup

Three models of trapezoidal free overfall channels were built and constructed from transparent perspex sheets, each model had 0.1m bed width and 3.7m length with different values of side-slope (m= 0.268, 0.577, and 1), see Fig. 2. In each model, the slope was changed four times as: S = zero, 0.0033, 0.01, and 0.02 (i.e., 0, 1/300, 1/100 and 1/50 respectively), based on a previous study [20]. For each bed, more than three hundred and eight strips of 10cm long and square cross section of 0.6cm × 0.6cm were manufactured. A transition, made from perspex, was connected to the upstream bed of the model in order to lead the flow over the model without disturbance and three screen type energy dissipators were fixed near the flume inlet to minimize water surface fluctuations in the trapezoidal channel. The testing program included ninety-six series of experiments. All models were fixed in a rectangular water tilting flume, having 5 m long, 0.3m wide and 0.45m in deep. The flow rate was measured by an electromagnetic flow meter with an accuracy of 0.01 l/s.

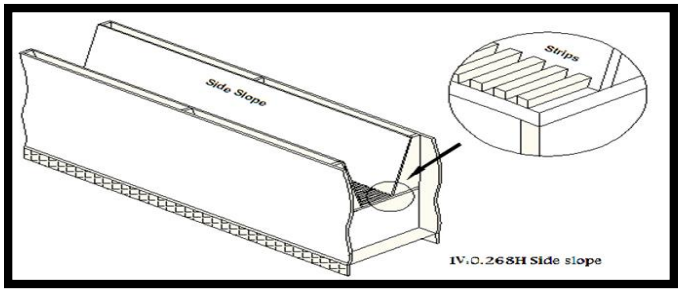

Figure 2. Trapezoidal channel model

B. Experimental Procedure Layout

Each model was installed and fixed at a distance (0.75m) from the downstream end of the flume and at a height 20cm above flume bed to create a vertical drop at the end of the channel. For each bed slope, eight different roughness patterns with various roughness elements spacing (center to center distance L =1.2 cm, 2.4 cm, 4.8 cm, 9.6 cm, 19.2 cm, 38.4 cm, 76.8 cm, and 153.6 cm) were tested, see Fig. 3. At the beginning of each experiment, water entered the inlet tank from a sump fed by a centrifugal pump. The flow rate was controlled manually by a butterfly valve which was located at the bottom of the flume on the delivery pipe and the delivery pipe was connected to the inlet tank. Different flow rates were allowed by gradually opening the valve until a desirable depth at the brink section of the channel was obtained. The brink depth (y_b) was varied from 2 cm to 7 cm during the eleven runs of each series. In each run, the brink depth was measured vertical to the channel bottom using a point gauge. The flow rate was recorded and the normal water depth was determined as the average value of many depths recorded upstream the brink section. A total of eight hundred sixty-four experiments were conducted during the experimental program through which side slope, bed slope and bed roughness of the channel were changed, see Fig. 4. Details of the experimental program are shown in Table. 1.

Figure 3. Rough bed model before testing

Figure 4. Rough bed model during a test run

TABLE 1. DETAILS OF THE EXPERIMENTAL PROGRAM.

Series No.	Model No.	Bed slope (S)	Roughness spacing (cm)	Number of runs
1-8	M1	S0	1.2, 2.4, 4.8, 9.6, 19.2, 38.4, 76.8 and 153.6	1-88
9-16		S1		89-176
17-24		S2		177-264
25-32		S3		265-352
33-40	M2	S0	1.2, 2.4, 4.8, 9.6, 19.2, 38.4, 76.8 and 153.6	353-440
41-48		S1		441-528
49-56		S2		529-616
57-64		S3		617-704
65-72	M2	S0	1.2, 2.4, 4.8, 9.6, 19.2, 38.4, 76.8 and 153.6	705-744
73-80		S1		745-784
81-88		S2		785-824
89-96		S3		825-864

In Table 1, S0 = horizontal bed slope, S1= bed slope = 0.0033, S2 = bed slope = 0.01, S3 = bed slope = 0.02, M1= model one of side slope (1V:0.268H), M2= model two of side slope (1V:0.577H), and M3=model three of side slope (1V:1H).

IV. RESULTS AND DISCUSSION

A. *Variation of Manning's Roughness Coefficient with Roughness Concentration*

For each run, the normal depth and discharge values were obtained and then the corresponding value of Manning's roughness coefficient (n) was calculated using Eq. (10). For each roughness pattern and different bed slopes, one average value of (n) was found. The average Manning's roughness coefficient values were obtained and tabulated in Table 2.

TABLE 2. AVERAGE VALUES OF MANNING'S ROUGHNESS COEFFICIENT FOR ALL ROUGHNESS PATTERNS.

(h/L)	M1	n	M2	n	M3	n	Average (n)
0.5	L1	0.0122	L1	0.0136	L1	0.0138	0.0132
0.25	L2	0.0146	L2	0.0158	L2	0.0166	0.0157
0.125	L3	0.0161	L3	0.0172	L3	0.0189	0.0174
0.0625	L4	0.0157	L4	0.0164	L4	0.0177	0.0166
0.03125	L5	0.0151	L5	0.0159	L5	0.0176	0.0162
0.01562	L6	0.0129	L6	0.0144	L6	0.0155	0.0143
0.00781	L7	0.0118	L7	0.0138	L7	0.0144	0.0133
0.00391	L8	0.0121	L8	0.0131	L8	0.0137	0.0130

The variation of average values of (n) with roughness concentration (h/L) for all patterns is plotted in Fig. 5. In this figure, it is interesting to realize that the maximum roughness appears to occur when the concentration of strips ($\lambda = h/L$) equal to 0.125 (when h = 0.6cm, and L= 4.8cm, this means patterns (L3)). The value of Manning's roughness coefficient for (λ = 0.125) is the highest among those of other concentrations which can be attributed to the distance between roughness elements.

For this particular concentration, the distance between roughness elements is neither so far apart in which the wake and vortex, at each element are completely developed and dissipated before the next element is reached nor the elements are placed so closed together in which the wake and vortex at each element will interfere with those developed at the following element. A similar conclusion was obtained by Mohammad [32] for strip and cub roughness elements, Noori [33] and Noori and Saeed [34] for prism roughness elements and that maximum bed roughness was observed at roughness concentration (λ = 0.125).

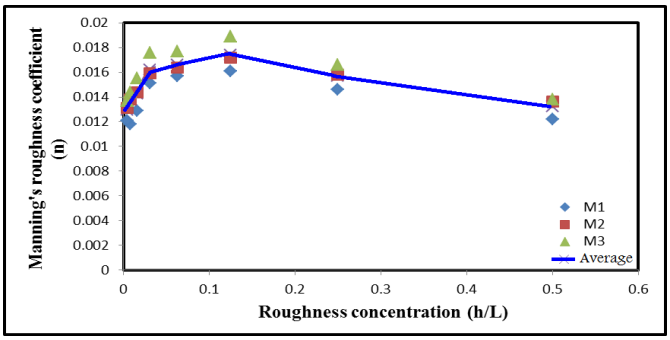

Figure 5. Variation of Manning's roughness coefficient with roughness concentration (h/L)

B. Variation of $\left(\frac{Qm^{1.5}}{\sqrt{gb^5}}\right)$ with $\left(\frac{my_b}{b}\right)$

As the pattern (L3) of all models showed the highest values of Manning's roughness (n), it is interesting to study the variation of $(Qm^{1.5}/\sqrt{gb^5})$ with (my_b/b) for each bed slope of this particular roughness pattern. The experimental results can be defined by simple power equation of the form:

$$\frac{Qm^{1.5}}{\sqrt{gb^5}} = a_1 \left(\frac{my_b}{b}\right)^{b1} \quad (17)$$

Values of constants (a_1) and (b_1) and the corresponding values of determination coefficient (R^2) were obtained for all bed slopes and tabulated in Table 3. The variation of $(Qm^{1.5}/\sqrt{gb^5})$ with (my_b/b) is plotted in Fig. 6 for different bed slopes of roughness pattern (L3). From Fig. 6, one may observe that values of $(Qm^{1.5}/\sqrt{gb^5})$ increase with the increase of (my_b/b) values. For other patterns, similar plots are presented somewhere else, Ibrahim [35].

TABLE 3. VALUES OF CONSTANTS (a_1) AND (b_1) AND (R^2) FOR DIFFERENT BED SLOPES OF ROUGHNESS PATTERN (L3).

Series No.	a_1	b_1	R^2
S0 L3	2.1474	1.6566	0.9982
S1 L3	2.3044	1.7033	0.9969
S2 L3	2.3509	1.7044	0.9979
S3 L3	2.4645	1.6983	0.9985

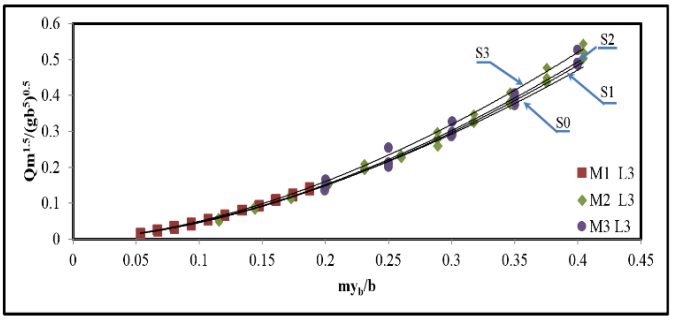

Figure 6. Variation of $(Qm^{1.5}/\sqrt{gb^5})$ with (my_b/b) for different bed slopes of roughness pattern (L3)

C. Variation of (my_b/b) with (my_c/b)

The variation of (my_b/b) with (my_c/b) was studied for each bed slope with roughness pattern (L3). The obtained experimental results for each bed slope can be defined by a simple linear equation of the following form:

$$\frac{my_b}{b} = a_2 \left(\frac{my_c}{b}\right) \quad (18)$$

in which, a_2 is a constant $= y_b/y_c$. Values of constant (a_2), the corresponding values of determination coefficient (R^2) and ranges of upstream Froude number ($F_r = V/\sqrt{gD}$, where: D = (A/T), A is the cross-sectional area, and T is the surface width of channel) were obtained for roughness pattern (L3 of $\lambda = 0.125$) and all bed slopes and tabulated in Table 4. The variations of (my_b/b) with (my_c/b) are plotted in Fig. 7 for all bed slopes and roughness pattern (L3). As depicted in these figures, the variation is linear and values of (my_b/b) increase with the increase of (my_c/b) values. It can be discerned from Table 4 that the ratio $(a_2 = y_b/y_c)$ decreases with increasing the slope with an average of 0.76 for sloping beds and 0.78 for horizontal beds with roughness concentration ($\lambda = 0.125$ *or pattern L3*). Similar plots for other patterns are presented somewhere else, Ibrahim [35].

TABLE 4. VALUES OF CONSTANT (a_2), (R^2) AND RANGE OF FROUDE NUMBER FOR DIFFERENT BED SLOPES AND ROUGHNESS PATTERN (L3)

Series No.	$a_2 = (y_b/y_c)$	R^2	Range of Froude No.
S0 L3	0.7816	0.9982	0.38-0.67
S1 L3	0.7776	0.9973	0.44-0.74
S2 L3	0.7691	0.9967	0.61-0.98
S3 L3	0.7433	0.9977	0.84-1.31

D. Variations of (y_b/y_c) with Bed Slope (S)

The slope of best fit line for the variation of (my_b/b) with (my_c/b) is the value of the ratio $(y_b/y_c = a_2)$. For each roughness pattern, the average value of (y_b/y_c) was obtained. The average values of (y_b/y_c) are correlated with channel bed slopes and the obtained relationship can be defined by polynomial equation of the form:

$$\frac{y_b}{y_c} = a_3 S^2 + b_3 S + c_3 \quad (19)$$

Values of constants a_3, b_3 and c_3 and the corresponding values of determination coefficient (R^2) for all roughness patterns are tabulated in Table 5. The variation of (y_b/y_c) with (S) is presented in Fig. 8 for all roughness patterns. Detailed examination of Table 5 and Fig. 8 shows that there is a polynomial relationship between the ratio (y_b/y_c) and slope (S) for each roughness pattern and values of (y_b/y_c) decrease with the increase of slope values. This can be attributed that as the slope increases the flow accelerates and the effect of flow lines curvature at brink (drop) decreases.

E. Variation of $(Qm^{1.5}/\sqrt{gb^5})$ with (my_b/b), and (S/n)

The functional relationship for the variation of $(Qm^{1.5}/\sqrt{gb^5})$ for the flow in trapezoidal channels of rough beds of different roughness patterns may be written as a function of (my_b/b), and the ratio of bed slope to Manning's roughness coefficient (S/n) for rough beds, as shown in Eq. (14):

To study the combined effect of (my_b/b) and (S/n) on $(Qm^{1.5}/\sqrt{gb^5})$, all experimental results of flow in trapezoidal channels of rough beds of different roughness patterns with different slopes were used as input data in the regression analysis program to obtain the following empirical power expression of the form:

$$\frac{Qm^{1.5}}{\sqrt{gb^5}} = 2.573 \left(\frac{my_b}{b}\right)^{1.711} \left(\frac{S}{n}\right)^{0.098} \quad (20)$$

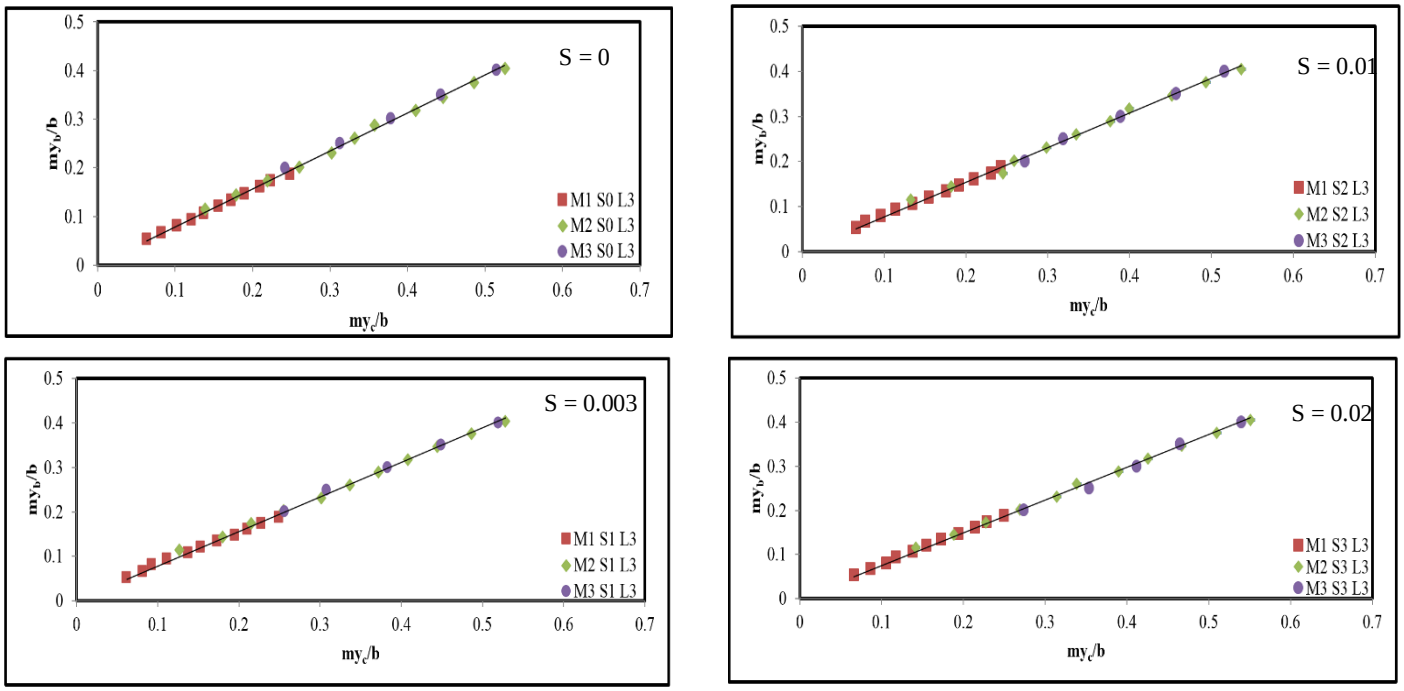

Figure 7. Variation of (my_b/b) with (myc/b) for different bed slopes and roughness pattern (L3)

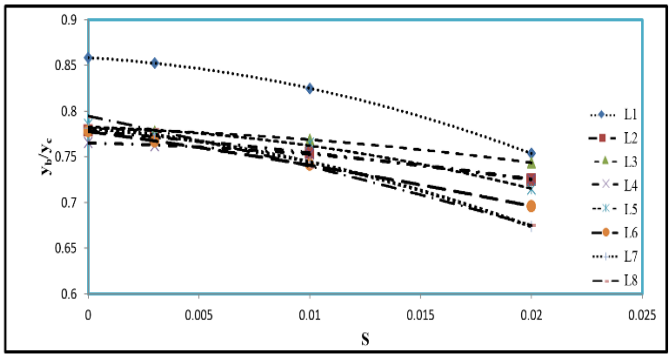

Figure 8. Variation of (y_b/y_c) with bed slopes (S) for different roughness patterns.

TABLE 5. VALUES OF CONSTANTS (a_3), (b_3), (c_3) AND (R^2) FOR BEDS OF DIFFERENT ROUGHNESS PATTERNS.

Roughness pattern	a_3	b_3	c_3	R^2
L1	-189.57	-1.4461	0.8583	1
L2	-25.423	-2.1724	0.7784	0.9998
L3	-63.815	-0.6032	0.781	0.9981
L4	-74.245	-0.4919	0.7649	0.9993
L5	-132.47	-0.7203	0.7824	0.9845
L6	-39.264	-3.3002	0.7775	0.9997
L7	-165.69	-2.0737	0.7813	1
L8	-47.216	-5.0366	0.7944	0.9998

Eq. (20) was obtained with determination coefficient (R^2) = 0.981 and standard error = 0.1278.

A comparison between values of Q observed experimentally and those predicted by Eq. (20) is shown in Fig. 9 showing quite good agreement.

The experimental data of flow in trapezoidal channels of rough and horizontal beds were used as input data in the same regression analysis program after considering the value of slope (S) to be zero; the following empirical power expression is obtained:

$$\frac{Qm^{1.5}}{\sqrt{gb^5}} = 2.173\left(\frac{my_b}{b}\right)^{1.684} \quad (21)$$

Eq. (21) was obtained with determination coefficient (R^2) = 0.985 and standard error = 0.1143.

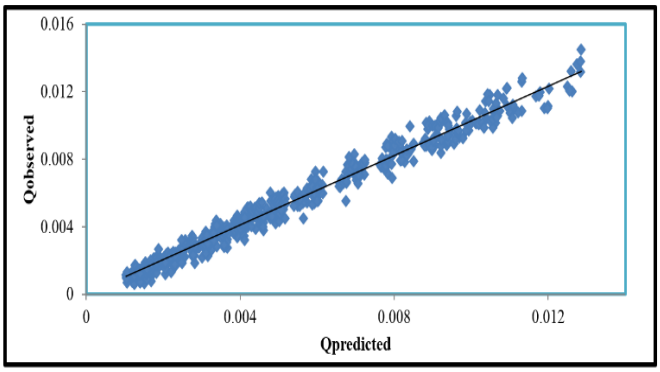

Figure 9. Variation of $Q_{observed}$ and $Q_{predicted}$

V. CONCLUSIONS

From the whole study, the following conclusions can be summarized:

- For each model of different bed slopes roughened with strips, the maximum roughness appears to occur when the concentration of strips ($\lambda = h/L$)equal to 0.125.

- The variation of $(Qm^{1.5}/\sqrt{gb^5})$ with (my_b/b) was found to be in the form of simple power equation. It was observed that the values of $(Qm^{1.5}/\sqrt{gb^5})$ increase with the increase of (my_b/b) values.
- The correlation between (my_b/b) with (my_c/b) was found to be linear for rough beds, different bed slopes and different roughness patterns. It was realized that values of (my_b/b) increase with the increase of (my_c/b) values with high determination coefficients.
- A polynomial relationship was found for the variation of (y_b/y_c) with bed slope (S) and the ratio (y_b/y_c) decreases with the increase of slope (S) for rough beds.
- The combined effect of (my_b/b), and (S/n) on $(Qm^{1.5}/\sqrt{gb^5})$ were studied for rough beds with different roughness patterns and different bed slopes. Two power empirical expressions were obtained. One of them for channels of different bed slopes (S = 0.0033, 0.01, and 0.02) with determination coefficient 0.981 and standard error = 0.1278. While, the second expression was for channels of horizontal beds with determination coefficient 0.985 and standard error = 0.1143.

VI. REFERENCES

[1] Dey, S.. "EDR in Circular Channels". Journal of Irrigation and Drainage Engineering, ASCE, Vol. 127, No. 2. 2001.

[2] Firat, C. E. "Effect of Roughness on Flow Measurements in Sloping Rectangular Channels with Free Overfall". M.Sc. Thesis METU, Ankara, February 2004.

[3] Rouse, H. ''Discharge Characteristics of the Free Overfall''. Civil Engineering, ASCE, Vol. 6, No.4. 1936.

[4] Delleur, J. W., Dodge, J. C. I., and Gent, K. N. '' Influence of Slope and Roughness on the Free Overfalls''. Journal of Hydraulic Engineering, ASCE, Vol. 82, N0. 4. 1956.

[5] Rajartnam, N., Muralidhar, D., and Beltaoss, S. '' Roughness Effects on Rectangular Free Overfall''. Journal of Hydraulic Engineering Division, ASCE, Vol. 102, No. 5. 1976.

[6] Davis, A. C., Jacob, R. P., and Ellett, B. G. S. "Flow Measurements in Sloping Channels with Rectangular Free Overfall". Journal of Hydraulic Engineering, ASCE, Vol.124, No. 7. 1998.

[7] Dey, S. "End Depth in Circular Channels". Journal of Hydraulic Engineering, ASCE, Vol. 124, No. 8. 1998.

[8] Dey, S. "End Depth in Steeply Sloping Rough Rectangular Channels". Indian Institute of Technology, Kharagpur, India, Sadhana, Vol. 25, Part 1. 1999.

[9] Dey, S., Kumar, D. N., and Singh, D. R. ''End-Depth in inverted Semicircular Channels: Experimental and Theoretical Studies". Indian Institute of Technology, Nordic Hydrology, Vol. 35, No. 1. 2002.

[10] Dey, S. "Free Overfall in Iverted Semicricular Channels". Journal of Hydraulic Engineering, ASCE, Vol. 129, No. 6. 2003.

[11] Dey, S. (2005). "End Depth in U-Shaped Channels: A Simplified Approach". *Journal of Hydraulic Engineering*, ASCE, Vol. 131, No. 6.

[12] Ferro, V."Theoretical End-Depth-Discharge Relationship for Free Overfall". Journal of Irrigation and Drainage Engineering, ASCE, Vol. 125, No. 1. 1999.

[13] Ahmad, Z. "Quasi-Theoretical End-Depth-Discharge Relationship for Rectangular Channels". Journal of Irrigation and Drainage Engineering, ASCE, Vol. 129, No. 2. 2003.

[14] Gue, Y., Zhang, L., Shen, Y., and Zhang, J. "Modeling Study of Free Overfall in a Rectangular Channel with Strip Roughness". Journal Hydraulic Engineering, ASCE, Vol. 134, No. 5. 2008.

[15] Tigrek, S., Firat C. E., and Ger, A. M. "Use of Brink Depth in Discharge Measurement". Journal of Irrigation and Drainage Engineering, ASCE, Vol.134, No. 89. 2008.

[16] Mohammed, M. Y., Al-Taee, A. Y., and Al-Talib, A. N. "Gravel Roughness and Channel Slope Effects on Rectangular Free Overfall". Damascus University Journal, Vol. 27, No. 1. 2011.

[17] Vatankhah, A. R. ''Direct Solution for Discharge in Generalized Trapezoidal Free Overfall'', Journal of Flow measurement and instrumentation, 29, 61-64. 2013.

[18] Diskin, M. H. ''End depth at a Drop in Trapezoidal Channels''. Journal of Hydraulic Division, ASCE, Vol. 87, No. 4. 1961.

[19] Hamid, H. I. Discussion of '' End Depth at a Drop in Trapezoidal Channels, by M. H. Diskin'', Journal of Hydraulic Engineering, ASCE, Vol. 88, N0. 1. 1962.

[20] Keller, R. J. and Fong, S. S."Flow Measurement with Trapezoidal Free Overfall". Journal of Irrigation and Drainage Engineering, ASCE, Vol. 115, No. 1. 1989.

[21] Terzidis, G., and Anastasiadou-Partheniou, L. Discussion of "Flow Measurements with Trapezoidal Free Overfall". By Robert J. Keller and Soon S. Fong. Journal of Irrigation and Drainage Engineering, ASCE, Vol. 116, No. 1. 1990.

[22] Replogle, J. A. Discussion of '' End Depth at a Drop in Trapezoidal Channels'', by M. H. Diskin''. Journal of Hydraulic Division, ASCE, Vol.88, No. 3. 1962.

[23] Rajaratnam, N, and Muralidhar, D. ''End Depth for Exponential Channels''. Journal of Irrigation and Drainage Engineering, ASCE, Vol. 90, No. 1. 1964.

[24] Gupta, R. D., Jamil, M., and Mohsin, M. "Discharge Prediction in Smooth Trapezoidal Free Overfall (Positive, Zero and Negative Slopes)". Journal of Irrigation and Drainage Engineering, ASCE, Vol. 119, No.2. 1993.

[25] Bhallamudi, S.M. "End Depth in Trapezoidal and Exponential Channels". Journal of Hydraulic Research, IAHR, Vol. 32, No .2, 1994. 219-232.

[26] Anastasiadou-Partheniou, L., and Hatzigiannakis, E. "General End-Depth-Discharge Relationship at Free Overfall in Trapezoidal Channel". Journal of Irrigation and Drainage Engineering, ASCE, Vol. 121, No. 2. 1995.

[27] Das, M. M., ''Open Channel Flow'', PHI Learning Private Limited, New Delhi – 110001. 2011.

[28] Schlichting, H. "Investigation of the Problem of Surface Roughness". NACA, TM 823. 1937.

[29] Morris, H. M."Design Methods for Flow in Rough Conduits". Journal of Hydraulic Division, ASCE, Vol. 85, No. 7. 1959.

[30] Gordienko, P. I. The Influence of Channel Roughness and Flow State on Hydraulic Resistances of Turbulent Flow". Journal Hydraulic Research, ASCE, Vol. 5, No. 4. 1967.

[31] Chow, V.T. "Open-Channel Hydraulics". International Edition, McGraw-Hill, Kogakusha, Ltd. 1959.

[32] Mohammed, N. A. "Hydraulic Resistance of Rough Steep Open Channels". M.Sc. Thesis, Department of Irrigation and Drainage Engineering, College of Engineering, University of Mosul, Iraq. 1989.

[33] Noori, B. M. A. "Artificial Roughness in Steep Open Channels". Journal of the Engineer, Scientific Society, Iraqi Engineering Union, Baghdad, Vol. 109, No. 1. 1992.

[34] Noori, B. M. A. and Saeed, M. S. "Hydraulic Resistance of Prismatic Roughness Elements in Steep Open Channels".Al. Rafidain Engineering Journal, Vol. 5, No. 1. 1997.

[35] Ibrahim, S. S. "Bed Stripped Roughness Effect on Flow Measurements in Trapezoidal Channels with Free Overfalls". M.Sc. Thesis, Duhok University. 2012.